

Charts for Estimating the Axial Shielding Factors for Triple-Shell Open-Ended Cylindrical Shields

Eugene Paperno, Hiroyuki Koide, and Ichiro Sasada

Abstract—Describing the shields with the number of shells greater than two differs from the previously done work in having a significant increase in the number of charts needed. To limit the number of charts, only the shields were examined that have the most-used exterior aspect ratio, namely, equal to 5. It was also assumed that all the shielding shells are made of the same material with an equal and relatively small thickness, which is a practical case as well. Since the three-shell structure does not allow much freedom for variations in the air gaps between the shells, only the shields having air gaps of 5% and 10% of the diameter of the outermost shell were considered. Finally, a set of charts was computed with the help of a standard ANSYS® software employing an FEM method. The charts are represented as logarithmic contour plots where the ratio of the inner to outer shells' lengths and permeability normalized to the thickness-to-diameter ratio of the outermost shell are independent variables; and the air gaps and ratio of the middle to outer shells' lengths are fixed parameters. The charts calculated allow one to quickly estimate the axial shielding factor and to clearly observe the effect of the shield's parameters on the axial shielding.

Index Terms—Axial (longitudinal) shielding factor, charts, magnetic shielding, open-ended cylindrical shields.

I. INTRODUCTION

THE PRESENT work extends [1], where the axial shielding factors (ASFs) for single- and double-shell open-ended cylindrical magnetic shields were calculated numerically and represented by special charts. The charts computed in [1] have shown themselves as an accurate and convenient reference tool, and attracted the interest of engineers and scientists who construct magnetic shields. On the other hand, axial shielding with multiple shells (three or more shells) provides much larger ASFs and is of a greater practical significance. It is important, therefore, to develop a new set of charts describing shielding with multiple shells. A further reason for extending [1] is that the existing theory [2]–[4] actually does not suggest a reliable analytical description of axial shielding with more than two open-ended shells. The results obtained in [2]–[4] are not in a close agreement with each other and with numerical calculations. Thus, either a time-consuming empirical approach or repetitive numerical simulations are used in practice to calculate the ASFs and optimize the axial performance of multiple-shell shields.

Manuscript received October 1, 2000.

E. Paperno is with the Department of Electrical and Computer Engineering, Ben-Gurion University of the Negev, Beer-Sheva 84105, Israel (paperno@ee.bgu.ac.il).

H. Koide and I. Sasada are with the Department of Applied Science for Electronics and Materials, Kyushu University, Kasuga-koen, Kasuga-shi, Fukuoka 816-850, Japan.

Publisher Item Identifier S 0018-9464(01)07109-6.

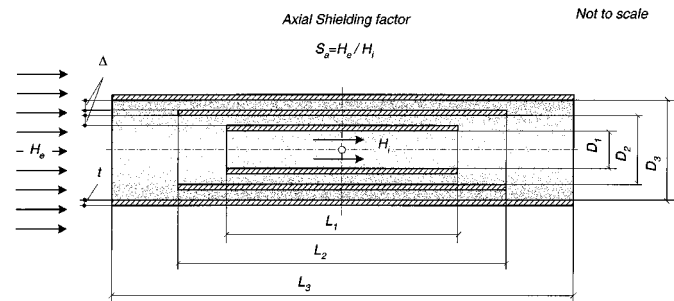


Fig. 1. A triple-shell open-ended cylindrical shield.

The present work is the first attempt of the authors to describe numerically, with the help of special charts, axial shielding with three open-ended cylindrical shells (see Fig. 1). The work that should be done in this respect differs from the previously done work [1] in having a significant increase in the number of charts needed. To limit the number of charts, we treat only the shields that have the most-used exterior aspect ratio, namely, equal to 5. (Triple- or multiple-shell open-ended shields with similar aspect ratio are in most common use since the effect of the openings significantly reduces the ASF for shorter shields.) We also assume that all the shielding shells are made of the same material with an equal and relatively small thickness, which is a practical case as well. Since the three-shell structure does not leave much freedom for variations in the air gaps between the shells, we consider only two types of shields that have air gaps of 5% and 10% of the diameter of the outermost shell. Finally, we compute a set of charts where the ratio of the inner to outer shells' lengths and normalized permeability are independent variables; and the air gaps and ratio of the middle to outer shells' lengths are fixed parameters (see Fig. 2).

II. COMPUTING THE CHARTS

To calculate the charts, a standard ANSYS® software package, employing a finite element method, was used. A 2-D axisymmetric model of the examined shields corresponds to a quadrant of Fig. 1. It is assumed that all the shielding shells are made of the same linear magnetic material with a permeability, μ , and an equal and relatively small thickness, t .

The length of the outermost shell, $L_3 = 100$ mm, its aspect ratio, $L_3/D_3 = 5 : 1$, and diameter-to-thickness ratio, $D_3/t = 100 : 1$, are identical for all the shields examined. The width of the air gaps between the shells, Δ , is a fixed parameter and takes the values 5% and 10% of D_3 . The ratio of the intermediate shell's length to the outer shell's length, L_2/L_3 , is another fixed parameter that varies from 0.5 : 1 to 1 : 1 in 0.1 increments. The

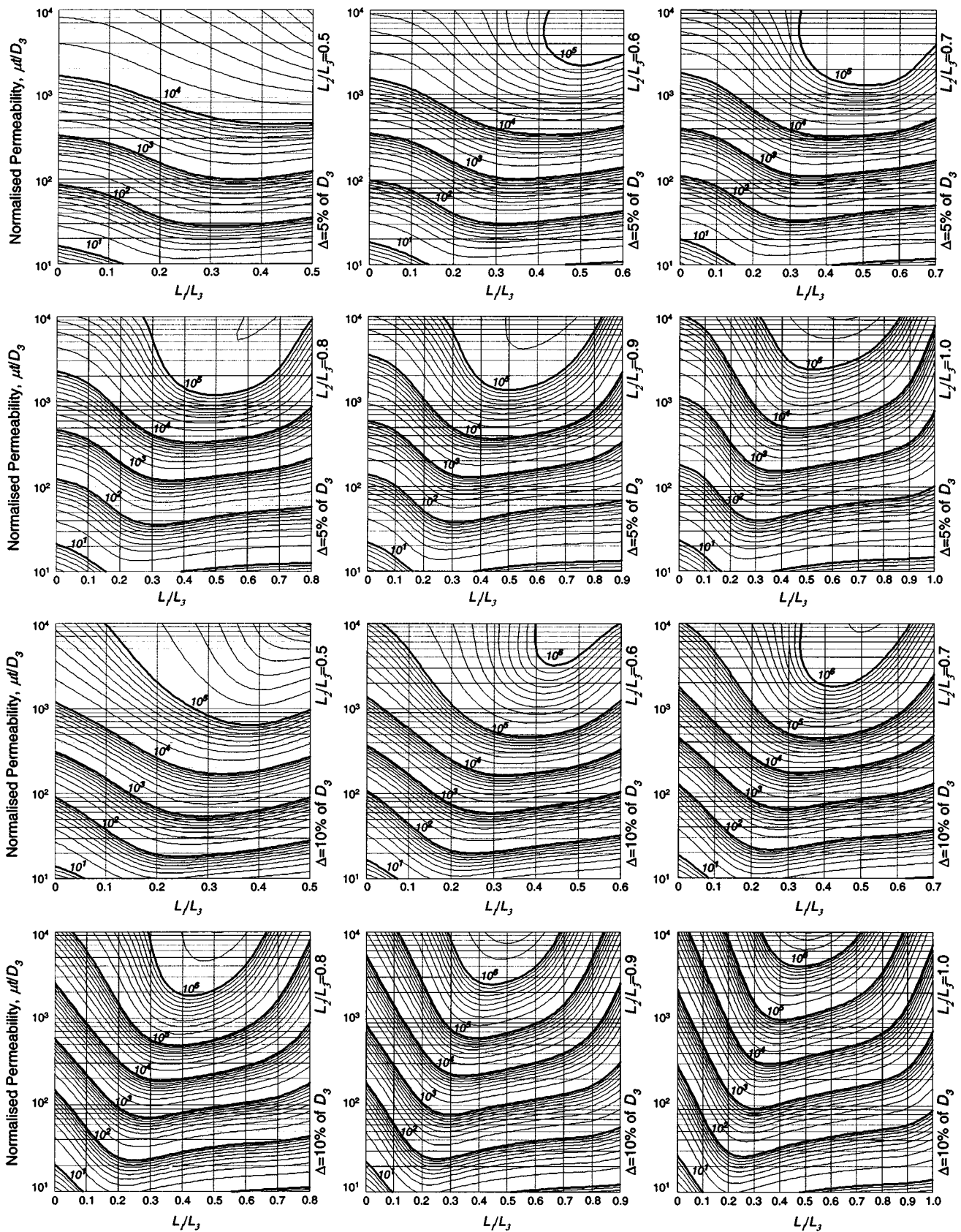


Fig. 2. Charts for estimating the axial shielding factors for triple-shell open-ended cylindrical shields.

ratio of the innermost shell's length to the outer shell's length, L_1/L_3 , is an independent variable that varies between 0 and the corresponding greatest value of the L_2/L_3 (see Fig. 2; L_1/L_2 is

always less than 1 : 1). The normalized permeability, $\mu_{\text{norm}} = \mu t/D_3$, is another independent variable that varies between 10^1 and 10^4 .

A layer of air surrounding the model was chosen wider than the exterior diameter of the shields by a factor of 9. Individual models were built for the shields of different geometries. The configuration of the numerical models is as follows, analysis type: linear static; element type: PLANE 53 (quadrangle shape, eight-nodes); mesh size: the finest, no. 1; standard smartsizing mesh level adjusted manually in order to have more than two layers of element covering the shields' cross sections; the aspect ratio of the elements was maintained in the range 1 : 2–1 : 1.

The following permeability values were selected for the calculations: $\mu = 10^3, 10^4, 10^5,$ and 10^6 , that corresponds to the following values of the normalized permeability: $\mu_{\text{norm}} = 10^1, 10^2, 10^3,$ and 10^4 . All the shields' models were exposed to a uniform axial magnetic field; and the ASF's were calculated at the center of each individual model. To simulate a uniform axial field (see Fig. 1) in the absence of the shield, Neumann type boundary conditions were implemented in the models.

In order to improve the resolution of the charts, the results of computations were interpolated by standard numerical procedures of MathCAD® and Mathematica® software. Finally, three-dimensional functions $S_a = f(L_1/L_3, \mu t/D_3)$ were represented as logarithmic contour plots for varied Δ and L_2/L_3 parameters (see Fig. 2).

Six upper charts in Fig. 2 represent triple-shell shields with the air gaps between the shells $\Delta = 5\%$ of D_3 ; and six lower charts represent the shields with $\Delta = 10\%$ of D_3 . The L_2/L_3 ratio for each set of charts increases from 0.5 : 1 to 1 : 1 in 1.0 increments (from left to right).

Given the charts, it is easy to observe both qualitatively and quantitatively the behavior of the ASF as being affected by the air gaps between the shielding shells, the shells' aspect ratios, and permeability. It allows a convenient way for optimizing the shield construction. For example, if the aim is to achieve the greatest ASF for a shield with $\mu_{\text{norm}} = 10^3$ then the following dimensional ratios should be chosen: $L_2/L_3 \approx 0.8, L_1/L_3 \approx 0.5$ for $\Delta = 5\%$ of D_3 and $L_2/L_3 \approx 0.7, L_1/L_3 \approx 0.4$ for $\Delta = 10\%$ of D_3 . The ASF achieved is $\sim 8 \cdot 10^4$ in the first case and $\sim 50 \cdot 10^4$ in the second case.

It is important to note that increasing the air gap width not only increases the ASF but also makes it more sensitive to the L_1/L_3 variable, especially for large permeabilities. It means that if for any reason—for instance, in order to increase the shielding area or to improve the residual field uniformity—the

shield dimensions are chosen different from those providing the greatest ASF then the drop in ASF will be more significant for the shield with larger Δ .

It is also interesting to note (see the chart in the top left hand corner of Fig. 2) that the greatest ASF for shields with $\mu_{\text{norm}} > 5 \cdot 10^2$ can be achieved when both inner shells are of an equal length. It means—as was a particular case of double-shell shields [1]—that it can be more important to elongate the innermost shell and decrease due to that the effect of the openings rather than to screen the ends of the innermost shell by a longer middle shell.

III. CONCLUSIONS

Axial shielding factors for triple-shell open-ended cylindrical magnetic shields were calculated numerically and represented by special charts. To limit the amount of charts, only the shields were examined that have the most-used exterior aspect ratio, namely, equal to 5; and only the shields having air gaps of 5% and 10% of the diameter of the outermost shell were considered. It was also assumed that all the shielding shells are made of the same material with an equal and relatively small thickness, which is a practical case as well. The above air gaps and the ratio of the middle to outer shells' lengths (0.5 : 1 to 1 : 1 in 0.1 increments) were chosen as fixed parameters; and the inner to outer shells' lengths ratio and normalized permeability were chosen as independent variables.

The charts computed allow a quick and relatively accurate estimating of the axial shielding factors in a wide range of the inner to outer shells' lengths ratio (from zero to the corresponding greatest value of the middle to outer shells' lengths ratio) and normalized permeability (from 10^1 to 10^4).

REFERENCES

- [1] E. Paperno, "Charts for estimating the axial shielding factors of open-ended cylindrical shields," *IEEE Trans. Magn.*, vol. 35, pp. 3940–3943, 1999.
- [2] A. Mager, "Magnetic shields," *IEEE Trans. Magn.*, vol. 6, pp. 67–75, 1970.
- [3] T. J. Sumner, J. M. Pendlebury, and K. Smith, "Conventional magnetic shielding," *J. Phys. D: Appl. Phys.*, vol. 20, pp. 1095–1101, 1987.
- [4] D. U. Gubser, S. A. Wolf, and J. E. Cox, "Shielding of longitudinal magnetic fields with thin, closely spaced, concentric cylinders of high permeability material," *Rev. Sci. Instrum.*, vol. 50, pp. 751–756, 1979.